EFFECTS OF CORROSION AND MECHANICAL DAMAGE ON PIPELINE RELIABILITY

Felipe Alexander Vargas Bazán, favb@sc.usp.br
André Teófilo Beck, atbeck@sc.usp.br
Department of Structural Engineering, São Carlos School of Engineering, University of São Paulo, Av. Trabalhador Sãocarlense 400, 13566-590, São Carlos, SP, Brazil

Abstract. *Mechanical damage (caused by third party interference) and corrosion are two of the three most significant causes of failure (spills) in oil and gas pipelines, according to international databases. Risk management for such facilities requires suitable models of corrosion growth with time and assessment of the influence of environmental and operating conditions on the likelihood of mechanical damage. This paper assembles state-of-the art failure models and uncertainty models for the reliability analysis of pipelines due to corrosion and mechanical damage. Both limit states are shown to be highly non-linear. Difficulties in solving the problem by means of the popular first order reliability method (FORM) are pointed out. Crude Monte Carlo simulation is used to evaluate failure probabilities in a pipeline case study. Consideration of pipelines as distributed systems is treated in a simplified manner. Frequency of occurrence of corrosion defects and mechanical damage incidents is collected from the literature in order to evaluate failure rates per kilometer for the distributed system.*

Keywords*: buried pipelines, reliability analysis, mechanical damage, corrosion*

1. INTRODUCTION

International databases reveal that mechanical damage due to third party interference and corrosion are two of the three most significant causes of failure (spills) in oil and gas pipelines. In European gas pipelines (EGIG, 2008), external interference is pointed out as the cause of 50% of the incidents. Material and construction defects appear in second place, with 16% of the incidents. Corrosion defects caused 15% of the incidents reported between 1970 and 2007.

With regard to oil pipelines, according to CONCAWE (2009), mechanical damage due to third party interference is the cause of 42% of the failures, 28% of the incidents are caused by mechanical failure and 19% are due to corrosion. If only pipelines operating in high temperatures are considered, the percentage of failures due to corrosion reaches 82%.

In a similar manner, UKOPA (2009) states that most pipeline spill incidents in England are originated by mechanical damage due to third party interference and by corrosion.

Risk management in pipeline operations requires suitable tools to model and predict probabilities of occurrence of spill events due to mechanical damage and corrosion. Probabilistic predictive tools make it possible to plan and manage maintenance practices, optimized in comparison to classical, deterministic standards. Predictive tools for pipeline reliability can also be used to investigate pipeline suitability at design stages.

The main purpose of this paper is to develop models for the prediction of pipeline reliability with respect to mechanical damage and corrosion failure modes. State-of-the-art models of mechanical damage and corrosion are employed.

Risk-based management of pipeline inspections may make feasible the operation of pipelines which would otherwise be retired. Additionally, risk reduction measures may be studied, such as increasing pipeline wall thickness and depth of cover.

Reports mentioned above (EGIG, 2008; CONCAWE, 2009; UKOPA, 2009) also indicate that occurrence of failures originated in corrosion defects has decreased in the last years, because of the monitoring by regular inspections (using instrumented pigs), and through maintenance practices. This shows the importance of risk management for buried pipelines.

2. FAILURE MODELS AND LIMIT STATE FUNCTIONS

2.1. Mechanical damage

Mechanical damage due to third party interference can cause pipe-wall dents and gouging (Fig. 1). A general approach to this problem is to conservatively treat the gouge as a crack-like defect and to consider the dent as a stress-modifier (Francis *et al.*, 2005).

The membrane and bending stress components due to denting are given, respectively, by:

$$\sigma_m = \sigma_h \left(1 - 1.8 \frac{D}{2R}\right) \tag{1}$$

and

$$\sigma_b = 10.2 \sigma_h \frac{D}{2t} \tag{2}$$

where: σ_h = hoop stress; D = depth of dent; R = inner radius of pipe; and t = pipeline wall thickness.

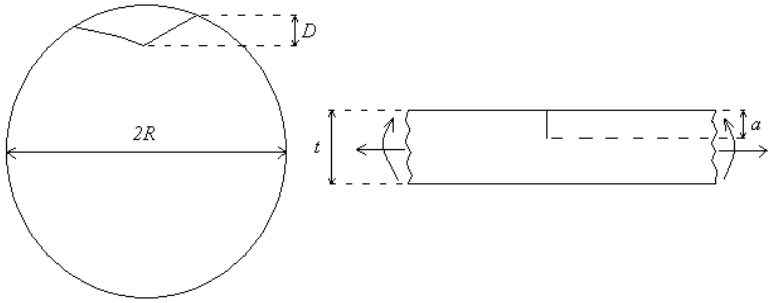

Figure 1. Dent gouge model details. Left: pipe with a dent; right: gouge modeled as a straight crack subjected to membrane and bending stresses (Francis *et al.*, 2005)

Hoop stress in a cylindrical pressure vessel is given by:

$$\sigma_h = \frac{pR}{t} \tag{3}$$

where: p = pipeline internal pressure.

In general, failure of steel structures containing crack-like defects occurs due to a combination of elastic fracture and plastic collapse. Accordingly, in this article the Level 1 elastic-plastic fracture mechanics model (R6 Procedure) presented in British Energy Generation Ltd. (2001) is employed. Hence, the limit state function for mechanical damage is (e.g. Beck & Melchers, 2004):

$$g_1 = \frac{\sigma_f}{\sigma_y}\left[\frac{8}{\pi^2}\ln\left\{\sec\left(\frac{\pi}{2}\frac{\sigma_f}{\sigma_y}\right)\right\}\right]^{-\frac{1}{2}} - \frac{K_I}{K_{IC}} \tag{4}$$

where: K_I = stress intensity factor; K_{IC} = fracture toughness (critical stress intensity factor); σ_f = far field stress at fracture; and σ_y = yield strength.

The relation between σ_f and σ_m is obtained from Francis *et al.* (2005):

$$\sigma_f = \frac{\sigma_m\left[1 - a/(M\,t)\right]}{1 - a/t} \tag{5}$$

where: a = depth of gouge; and M = Folias factor.

Taking into account the effect of the gouge length, Folias factor is given by:

$$M = \left[1 + 0.26\left(\frac{L}{\sqrt{Rt}}\right)^2\right]^{\frac{1}{2}} \tag{6}$$

where: L = length of gouge.

For calculating the stress intensity factor, a rectangular-shaped gouge with dimensions a and L is considered. It is assumed that the length of the gouge is much greater than its depth. Hence, the gouge can be considered two-dimensional and the fracture is determined only by gouge depth and not by gouge length.

According to Francis *et al.* (2005), both membrane and bending stresses – Eqs. (1) and (2), respectively – can contribute to fracture, and the stress intensity factor may be expressed in the form:

$$K_I = \left(\sigma_m Y_m + \sigma_b Y_b\right)\sqrt{\pi\, a} \tag{7}$$

where $Y_m(a/t)$ and $Y_b(a/t)$ are normalized stress intensity compliance functions. In accordance with the assumption above, these functions are given, conservatively, by the stress intensity factors for an infinitely long (two-dimensional) edge crack in a strip subjected to remote tension and bending (Rooke and Cartwright, 1976; Cheng and Finnie, 1988):

$$Y_m = 1.12 - 0.23(a/t) + 10.6(a/t)^2 - 21.7(a/t)^3 + 30.4(a/t)^4 \tag{8}$$

$$Y_b = 1.12 - 1.39(a/t) + 7.32(a/t)^2 - 13.1(a/t)^3 + 14(a/t)^4 \tag{9}$$

2.2. Corrosion

For corrosion defects the limit state function suggested by DNV-RP-F101 (2004), given by the following expression, is used:

$$g_2 = P_{cap} - p \tag{10}$$

where: P_{cap} = burst pressure capacity.

The burst pressure capacity is given by:

$$P_{cap} = X_M \frac{2t \cdot \sigma_u}{(2R_0 - t)} \frac{(1 - d/t)}{\left(1 - \dfrac{d/t}{Q}\right)} \tag{11}$$

where: R_0 = outer radius of pipe; X_M = model uncertainty random variable; σ_u = ultimate tensile strength; d = maximum depth of corrosion defect; and Q = defect length correction factor.

Equation (11) is a simplified version, suggested for practical use, of a more elaborate expression for the burst pressure capacity developed by DNV-RP-F101 (2004). This original study was based on a large number of finite element analyses and a series of full scale burst tests.

The length correction factor in Eq. (11) is calculated as:

$$Q = \sqrt{1 + 0.31\left(\frac{l}{\sqrt{2R_0 t}}\right)^2} \tag{12}$$

where: l = longitudinal length of corrosion defect.

Figure 2 shows a scheme of an irregular metal loss defect caused by corrosion. For simplicity, an equivalent rectangular defect is used in this study.

Corrosion defects grow with time. In this study, a linear growth model for the maximum defect depth is assumed. Therefore, d grows with a constant rate v. It is assumed that corrosion defects grow from the time the pipeline is commissioned. Hence, the time-dependent burst pressure capacity, Eq. (11), becomes:

$$P_{cap}(\tau) = X_M \frac{2t \cdot \sigma_u}{(2R_0 - t)} \frac{(1 - v\,\tau/t)}{\left(1 - \dfrac{v\,\tau/t}{Q}\right)} \tag{13}$$

where: τ = time elapsed since pipeline commissioning; and v = rate of growth of defect depth.

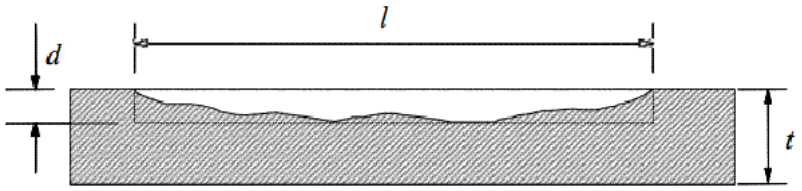

Figure 2. Corrosion defect dimensions (DNV-RP-F101 2004)

3. UNCERTAINTY MODELS

In this section the statistical models used to quantify uncertainties in problem parameters are described.

Pipe outer diameter ($2R_0$) was assumed deterministic and equal to its nominal value. This assumption is based on Jiao *et al.* (1995), which indicate that the variability of the actual pipe diameter is negligible.

3.1. Mechanical damage

The following are assumed as the uncertain variables of the mechanical damage limit state function. Eq. (4):

1 internal operating pressure;
2 wall thickness;
3 yield strength;
4 fracture toughness;
5 gouge length;
6 gouge depth and
7 denting force.

Internal pressure (p) is the only load considered and is represented by a Gumbel distribution having a mean equal to 1.05 times the MAOP (maximum allowable operating pressure) and a coefficient of variation (CoV) of 3% (DNV-RP-F101, 2004).

Wall thickness (t) is represented as a normal variable with mean equal to the nominal value and a CoV of 3% (DNV-RP-F101, 2004).

Yield strength (σ_y) of pipeline steel is assumed to follow a lognormal distribution model, with mean 8% larger than the SMYS (specified minimum yield stress) and a CoV of 4% (Jiao *et al.*, 1995).

In the pipeline industry, it is not common to measure fracture toughness (K_{IC}) directly. It is generally determined from impact tests (Charpy) by means of an empirical correlation to Charpy fracture energy (J_{IC}). Hence, sufficient test data to postulate a statistical distribution for this variable is rare in the literature. In this paper, a Weibull distribution is arbitrarily assumed for fracture toughness.

As stated in section 2.1, it is assumed that third-party interference causes denting and gouging of the pipeline. This kind of damage is caused by machinery such as excavators and farm machinery. Distributions for denting and gouging parameters (i.e. dent depth, gouge length and gouge depth) were drawn from UKOPA fault records.

Gouge length (L) was represented by a Weibull distribution with shape value (β) of 0.84 and scale parameter (u_1) of 183.6 mm.

Gouge depth (a) was modeled by a Weibull distribution with shape value (β) of 0.63 and scale parameter (u_1) of 0.73 mm.

Dent depth (D) is not modeled directly because, for a given impact force, it depends on pipe dimensions, material properties and operating pressure. Historical data is insufficient to estimate dent depth distributions for individual combinations of these variables. Francis *et al.* (2002) suggest the following empirical relationship:

$$D = \left[\frac{F}{0.49 \cdot \sqrt{\left(t + \frac{1.4\,pR}{1.15\sigma_y} \right) \left(80 t \sigma_y \right)^{\frac{1}{4}}}} \right]^{2.38} \tag{14}$$

where: F = denting force.

Francis *et al.* (2002) combined Eq. (14) with historical data to obtain a probability distribution for F. This is a Weibull distribution with shape value (β) of 2.12 and scale parameter (u_1) of 55 kN.

Table 1 summarizes statistical distributions of the mechanical damage limit state random variables.

Table 1. Mechanical damage limit state random variables.

Variable	Distribution	Parameter 1[(1)]	Parameter 2[(1)]
p	Gumbel	μ = 1.05 MAOP	CoV = 3%
t	Normal	$\mu = t_n$	CoV = 3%
σ_y	Lognormal	μ = 1.08 SMYS	CoV = 4%
K_{IC}	Weibull	μ = 100 MPa·m$^{1/2}$	CoV = 5%
L	Weibull	β = 0.84	u_1 = 183.6 mm
a	Weibull	β = 0.63	u_1 = 0.73 mm
F	Weibull	β = 2.12	u_1 = 55 kN

(1): μ = mean value; CoV = coefficient of variation; β = shape parameter; u_1 = scale parameter; t_n = nominal wall thickness.

With the models described above, the probability of failure given that a single mechanical damage incident has occurred can be calculated. In this paper, the First Order Reliability Method (FORM) and direct Monte Carlo simulation are used (Ditlevsen and Madsen, 1996; Melchers, 1999).

The limit state function for mechanical damage, Eq. (4), allows one to evaluate a failure probability that is conditional to a mechanical hit incident. The actual reliability of the distributed pipeline also depends on the frequency with which incidents can be expected to occur. This frequency of hits has to be estimated from historical data, taking into account the installation and location conditions for the pipeline (depth of cover, nature of environment, use of warning and protection systems, and surveillance interval). Changes in these factors are likely to affect the frequency of hits and, therefore, the pipeline failure frequency.

The failure frequency for mechanical damage, η_{f1}, is then given by:

$$\eta_{f1} = \eta_h \, P_{f1} \tag{15}$$

where: η_h = frequency of hits; and P_{f1} = probability of failure conditional to a single incident/hit.

Frequency of hits and failure frequency are usually given for a reference pipeline length (e.g. 1 km) and a reference period (e.g. one year), i.e. per km·year.

Finally, the time-dependent failure probability (or rate per km) due to mechanical damage can be calculated as (Melchers, 1999):

$$P_{fmd}(\tau) = 1 - \exp\left(-\eta_{f1}\,\tau\right) \tag{16}$$

where $P_{fmd}(\tau)$ is usually expressed per km and represents the accumulated probability of failure for a given time period and pipeline length.

3.2. Corrosion

The following are assumed as the uncertain variables of the corrosion limit state function (Eq. (10)):

1 internal operating pressure;
2 wall thickness;
3 ultimate tensile strength;
4 defect length;
5 defect maximum depth growth rate and
6 model uncertainty.

The first two parameters were already described in section 3.1, since they are common to both mechanical damage and corrosion limit state functions.

For distributions of ultimate tensile strength (σ_u), defect length (l) and model uncertainty factor (X_M), recommendations of DNV-RP-F101 (2004) are followed. For growth rate (v) of maximum defect depth, a lognormal distribution with parameters based on CSA Z662-07 (2007) and Zhou (2010) is adopted. Table 2 presents statistical distributions of the corrosion limit state random variables.

Table 2. Corrosion limit state random variables.

Variable	Distribution	Parameter 1[(1)]	Parameter 2[(1)]
p	Gumbel	μ = 1.05 MAOP	CoV = 3%
t	Normal	$\mu = t_n$	CoV = 3%
σ_u	Normal	μ = 1.09 SMTS	CoV = 3%
l	Normal	$\mu = 25 \cdot$ mm[(2)]	σ = 19.5 mm[(2)]
v	Lognormal	μ = 0.15 mm/yr	CoV = 50%
X_M	Normal	μ = 1.05	CoV = 10%

(1) : μ = mean value; CoV = coefficient of variation; σ = standard deviation;
t_n = nominal wall thickness; SMTS = specified minimum tensile strength.
(2) : Estimated values

With the models described above, the probability of failure for a single corrosion defect can be calculated. Since corrosion defects grow in size with the passing of time, the probability of failure for a single corrosion defect increases with the time elapsed since pipeline commissioning.

The number of corrosion defects (or rate of defects per km of pipeline and year) also have to be estimated from historical data or from line inspections. This rate may increase in time as new corrosion defects will appear during the pipeline's life.

The predicted corrosion failure frequency, η_{f2}, is given by:

$$\eta_{f2}(\tau) = \eta_d(\tau) P_{f2}(\tau) \tag{17}$$

where: $\eta_d(\tau)$ = frequency of corrosion defects per km·year; and P_{f2} = probability of failure for a single corrosion defect.

For corrosion, the failure frequency, Eq. (17), is time-variant, hence the accumulated, time-dependent failure rate is calculated as (Melchers, 1999):

$$P_{fc}(\tau) = 1 - \exp\left(-\int_0^{\tau} \eta_{f2}(\xi) d\xi \right) \tag{18}$$

where $P_{fc}(\tau)$ is usually expressed per km and represents a cumulative probability of failure for a reference pipeline length.

4. NUMERICAL EXAMPLE

In this section, a numerical example is presented to illustrate the methodology described above for structural reliability analysis of pipelines under mechanical damage and corrosion.

A grade X42 steel pipeline is considered, with the following main features:

1 nominal outside diameter: 16 in (406.4 mm);
2 nominal wall thickness: 6.4 mm;
3 MAOP: 940 psi (6.5 MPa);
4 SMTS: 60,000 psi (414 MPa) and
5 SMYS: 42,000 psi (290 MPa).

4.1. Condicional P_f for mechanical damage

The mechanical damage limit state equation, Eq. (4), is illustrated in Fig. 3 for the nominal pipeline parameters considered herein. The R6 failure assessment diagram is showed in terms of variables (K_r, S_r), where $K_r = K_I / K_{IC}$ and $S_r = \sigma_f / \sigma_y$.

The nominal loading point (K_r, S_r) is calculated from nominal values of design variables, namely (in same order as illustrated in Tab. 1, and with subscript n indicating nominal value): p_n = MAOP; t_n; σ_{yn} = SMYS; K_{Icn} = 100 MPa·m$^{1/2}$; L_n = 183.6 mm; a_n = 0.73 mm; and F_n = 55 kN. This nominal load point is illustrated in Fig. 3a.

Load trajectories for variables of interest can also be observed in Fig. 3. Figs. 3b-d show such trajectories for gouge depth, denting force and internal pressure, respectively. The load trajectories help one to understand the roles of these variables in the mechanical damage limit state. Larger denting forces (Fig. 3c), for example, reduce stresses in the dented pipeline, but increase stress intensity factors in bending, leading to a more elastic (brittle) fracture. Increases in pipeline pressure (Fig. 3d), on the other hand, lead to more ductile failures.

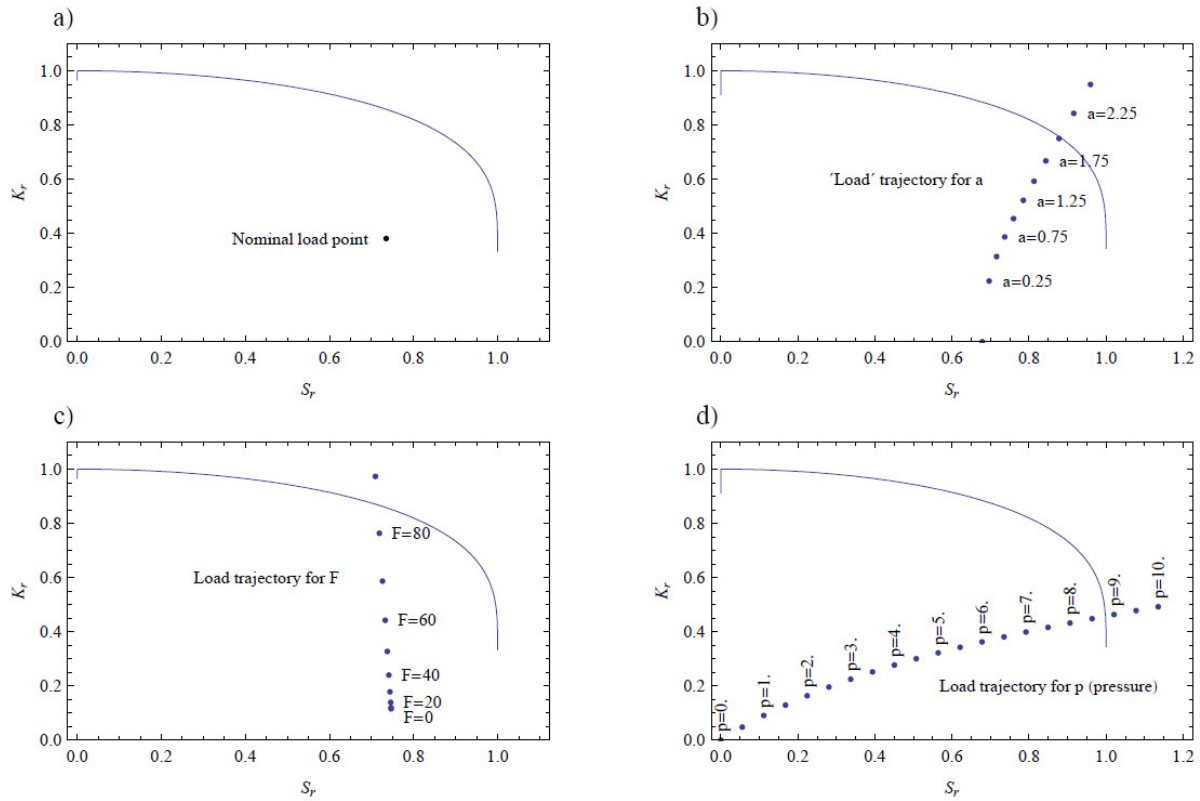

Figure 3. R6 failure assessment diagram for mechanical damage limit state, nominal load point (a), and "load trajectories" for varying gouge depth (b), denting force (c) and internal pressure (d).

Reliability analyses were performed, in order to calculate probabilities of failure conditional to a single mechanical damage incident. A first-order approximation (FORM) yielded $P_{f1} \approx 0.134$, and revealed that denting force (F) and crack (gouge) depth (a) are the random variables with most contribution to failure probability. Figure 4 illustrates level curves of the joint probability density function for these two variables, as well as the limit state function and the FORM most probable point (MPP). A sharp curvature of the limit state function can be observed, in terms of these two variables. Due to this curvature, the first-order result is not accurate, and (crude) Monte Carlo simulation was performed, yielding $P_{f1} \approx 0.1$. This value is used in the subsequent analysis.

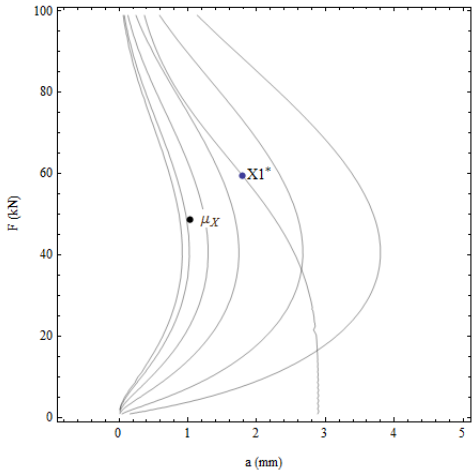

Figure 4. Limit state function for mechanical damage and joint probability density function (level curves) for variables denting force (F) and gouge depth (a).

4.2. Condicional P_f for corrosion

Figure 5 illustrates burst-pressure trajectories in terms of time for different corrosion rates ($v = \mu_v$ and $v = \mu_v \pm \sigma_v$). It is observed that the problem is highly dependent on the corrosion rates, partly because the coefficient of variation (CoV) of corrosion rate is large (50%).

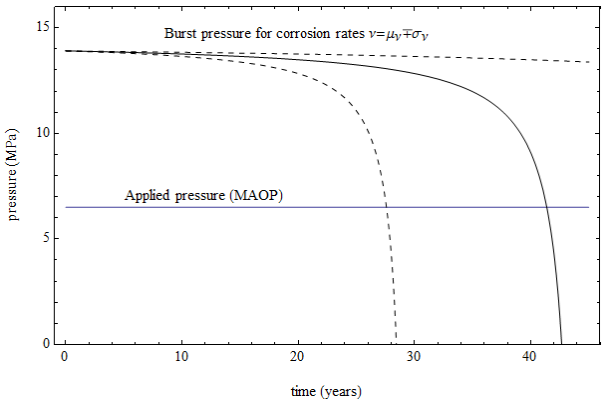

Figure 5. Nominal burst pressure capacity as a function of time elapsed since pipeline commissioning. Mean and lower/upper trajectories for corrosion rates $v = \mu_v$ and $v = \mu_v \pm \sigma_v$.

The probability of failure given a single corrosion defect was evaluated, as a function of time. This was initially performed by FORM, but some instability (and high curvature) of the limit state functions was observed (Fig. 6). For τ = 11 years or smaller, model error (X_M) is the dominating variable, and the most probable failure point (MPP) is obtained for small values of both model error and corrosion rate random variables. For τ = 13 years or larger, corrosion rate (v) is the dominating variable, and the most probable failure point (MPP) is obtained for near-unitary model errors but for very large corrosion rates. The transition between these two conditions ($11 < \tau < 13$) produces sharp oscillations in the numerical algorithm used to locate the MPP points. Moreover, the sharp curvatures observed in the limit state function (Fig. 6) make first-order results inaccurate, hence crude Monte Carlo simulation had to be used in the evaluation of failure probabilities.

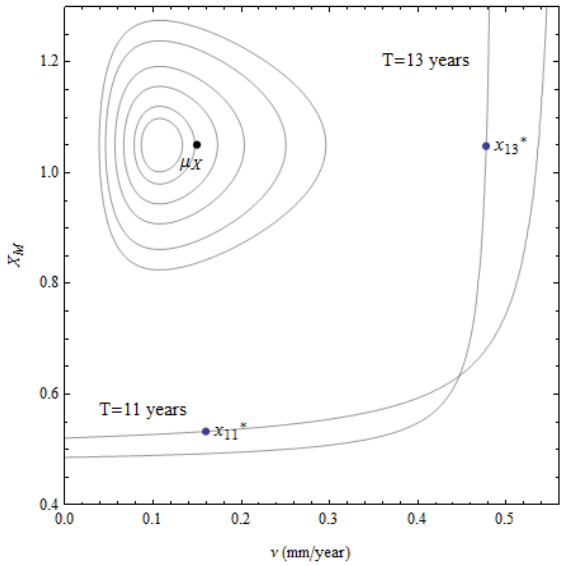

Figure 6. Limit state functions for corrosion and most-probable (MPP) failure points (x_{11}* and x_{13}*) for 11 and 13 years, in terms of corrosion rate (v) and model error (X_M).

The sharp transition in MPP points for τ = 11 and τ = 13 years can also be observed in Fig. 7, where the most probable (MPP) paths to failure are illustrated. It can be observed that the MPP path to failure for τ = 11 years starts at a very low "realization" of the model error random variable, and requires little defect growth until failure. On the other hand, for τ = 13 years the MPP path to failure starts near the mean burst pressure ($X_M \approx 1$), but the defect grows very

fast due to a large "realization" of the corrosion rate v. For both paths, the burst pressure drops to the MPP applied pressure for $\tau = 11$ and $\tau = 13$ years, respectively.

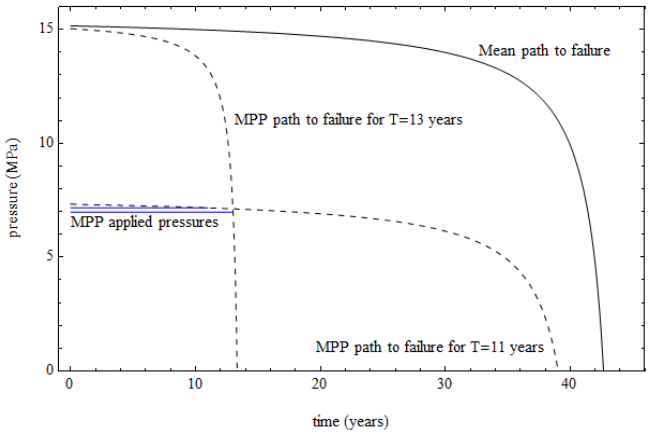

Figure 7. Burst pressure trajectories as a function of time: mean path to failure and most probable (MPP) paths to failure for $\tau = 11$ and 13 years.

Given the difficulties just described, the conditional probabilities of failure due to a single corrosion defect, as a function of time, were evaluated by crude Monte Carlo simulation, using 10^5 samples. For 11 and 13 years, in particular, these where found to be: $P_{f2}(\tau=11)\approx 1.45\times10^{-3}$ and $P_{f2}(\tau=13)\approx 4.03\times10^{-3}$. Using the FORM approximation, the same failure probabilities had been evaluated as $P_{f2}\approx 1.05\times10^{-7}$ and $P_{f2}\approx 3.45\times10^{-3}$, respectively. This shows that the difficulties with the FORM solution are not just about instability in finding the design point, but also with the linear approximation of the limit state function.

4.3. Failure probabilities for distributed pipelines

The failure probabilities calculated above are conditional to the occurrence of a single mechanical damage incident or to a single corrosion defect. Pipelines are distributed systems, whose overall failure probabilities depend on the length of pipeline as well as on the frequency of hits (hits per km·year) and the mean number of corrosion defects per km·year.

In the present example, statistics obtained by UKOPA (2009) were assumed for the frequency of hits: $\eta_h = 5\times10^{-5}$ hits per km·year (assumed time invariant). Hence, from Eq. (15), $\eta_{f1} \approx 5\times10^{-6}$ (failure rate per km·year). The failure probability (or rate per km) is accumulated over a given time-period using Eq. (16).

From the same UKOPA (2009) report, the frequency of occurrence of corrosion defects is obtained as $\eta_d = 5\times10^{-5}$ defects per km·year. This rate could typically increase in time, as new defects appear in the pipeline. In the long run, however, and considering the effect of line inspections and repair, this rate could be assumed to remain constant. Hence, failure probabilities due to corrosion are evaluated from Eqs. (17) and (18).

Figure 8 compares the evolution in time of the (time-integrated) failure rates (per km) for mechanical damage and corrosion. The rate of failure due to mechanical damage only increases due to integration over time, since the rate over time is constant. On the other hand, the rate of failure due to corrosion increases much sharply, as conditional failure probabilities also increase in time due to the growth of corrosion defects. The trend illustrated in Fig. 8 does not include the effects of line inspection and repair, which should be included in a future extension of the present study.

5. FINAL REMARKS

This article assembled failure models and uncertainty models for the reliability analysis of buried pipelines with respect to failure due to mechanical damage (third-party interference) and due to corrosion. These are two of the three most significant causes of failure (spills) in oil and gas pipelines.

Limit states and uncertainty models were based on international references and reflect the current state-of-the-art of the field. Some issues related to the high-nonlinearity and concavity of the limit state functions for mechanical damage and corrosion were presented and discussed. It was shown that the FORM solution is not suitable for these problems, and hence Monte Carlo simulation was used in the present study.

This is an ongoing research project. In this first approach to the problem, little attention was dedicated to the actual modeling of the distributed pipeline system, nor to the effects of inline inspection and repair. These issues will be addressed in a continuation of the present study.

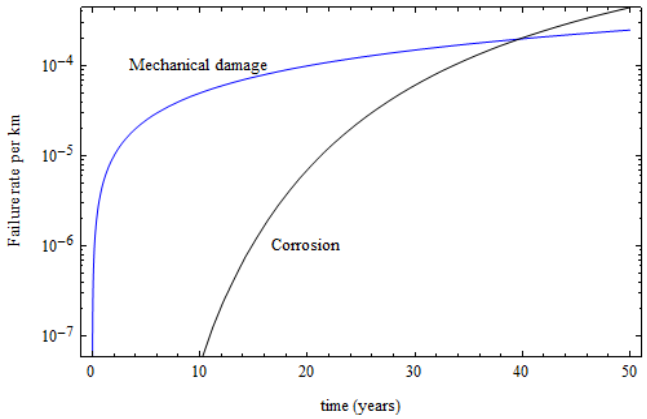

Figure 8. Failure rates (per km) for a pipeline subjected to mechanical damage and corrosion, as functions of time.

6. ACKNOWLEDGEMENTS

Sponsorship of this research project by the Brazilian National Council for Higher Degree Education (CAPES) and by the Brazilian National Council for Research and Development (CNPq) is greatly acknowledged.

7. REFERENCES

Beck, A.T. and Melchers, R.E., 2004. "Overload failure of structural components under random crack propagation and loading - a random process approach". *Structural Safety*, Vol. 26, No. 4, pp. 471-488.

British Energy Generation Ltd., 2001. *Assessment of the integrity of structures containing defects*. R6 Revision 4, British Energy Generation Ltd., UK.

Cheng, W. and Finnie, I., 1988. "K_I solutions for an edge-cracked strip". *Engineering Fracture Mechanics*, Vol. 31, No. 2, pp. 201-207.

CONCAWE, 2009. *Performance of European cross-country oil pipelines: statistical summary of reported spillages in 2007 and since 1971*. Brussels, Belgium.

CSA Z662-07, 2007. *Oil and gas pipeline systems*. Canadian Standard Association, Mississauga, Ontario, Canada.

Ditlevsen, O. and Madsen, H.O., 1996. *Structural reliability methods*. John Wiley & Sons, Chichester, England.

DNV RP-F101, 2004. *Recommended practice - Corroded pipelines*. Det Norske Veritas, Høvik, Norway.

EGIG, 2008. *Gas pipeline incidents - 7th Report of the European Gas Pipeline Incident Data Group: 1970-2007*.

Francis, A., Gardiner, M. and McCallum, M., 2002. "Life extension of a high pressure transmission pipeline using structural reliability analysis". In *4th International Pipeline Conference*. Calgary, Alberta, Canada, September 29-October 3.

Francis, A., Jandu, C.S., Andrews, R.M., Miles, T.J. and Chauhan, V., 2005. "Development of a new limit state function for the failure of pipelines due to mechanical damage". In *15th Biennial PRCI/EPRG Joint Technical Meeting on Pipeline Research*. Orlando, USA, May.

Jiao, G., Sotberg, T. and Igland, R., 1995. *SUPERB 2M - statistical data: basic uncertainty measures for reliability analysis of offshore pipelines*. SUPERB JIP report.

Melchers, R.E., 1999. *Structural reliability analysis and prediction*. 2nd edition. John Wiley & Sons, Chichester, England.

Rooke, D.P. and Cartwright, D.J., 1976. *Compendium of stress intensity factors*. HMSO, London, England.

UKOPA, 2009. *Pipeline product loss incidents - 6th Report of the UKOPA Fault Database Management Group*. United Kingdom Onshore Pipeline Association.

Zhou, W., 2010. "System reliability of corroding pipelines". *International Journal of Pressure Vessels and Piping*, Vol. 87, No. 10, pp. 587-595.

8. RESPONSIBILITY NOTICE

The authors are the only responsible for the printed material included in this paper.